Synergistic Spin-Ligand Effects on the Oxygen Reduction Activity of FePPc Electrocatalyst

Ya Jin[1,2,3], Mingyuan Yu[1,2,3], Erjun Kan[1,2,3], Cheng Zhan[1,2,3]*

[1]School of Physics, Nanjing University of Science and Technology, Nanjing 210094, China

[2]MIIT Key Laboratory of Semiconductor Microstructure and Quantum Sensing, Nanjing University of Science and Technology, Nanjing 210094, China

[3]Engineering Research Center of Semiconductor Device Optoelectronic Hybrid Integration in Jiangsu Province, Nanjing 210094, China

*Corresponding author: Cheng Zhan

E-mail dress: czhan@njust.edu.cn

Gibbs free energy calculation at constant potential.

The four-step proton-coupled electron transfer process in OER and ORR is defined as follows:

$$* + O_2 + H^+ + e^- \rightarrow *OOH \quad \text{(S1)}$$

$$*OOH + H^+ + e^- \rightarrow *O + H_2O \quad \text{(S2)}$$

$$*O + H^+ + e^- \rightarrow *OH \quad \text{(S3)}$$

$$*OH + H^+ + e^- \rightarrow * + H_2O \quad \text{(S4)}$$

where * represent the catalytic site. The forward arrow indicates OER, and the directional arrow indicates ORR. At U=0V vs. SHE, the free energy of proton-electron pair was set as the chemical potential of $\frac{1}{2}H_2$,[1] and then its free energy at any potential U can be expressed as:

$$G_{H^+}(U) + G_{e^-}(U) = G_{H^+}(U) - e*(4.6 + U) = \frac{1}{2}G_{H_2} - e*U \quad (S5)$$

and the G_{H_2} can be calculated by:

$$G_{H_2} = E_{H_2} + E_{ZPE} - T*S + C_p(T) \quad \text{(S6)}$$

the E_{H_2} was calculated by DFT, E_{ZPE} is zero-point energy obtained from vibration calculation at T = 298.15 K and P = 1 bars. S and $C_p(T)$ is standard entropy and heat capacity taken from

thermodynamic table. For liquid water calculations, we consider the chemical potential of liquid water is equal to the chemical potential of water in the gas phase at T = 298.15 K and P = 0.035 bars.[2] Since the energy of O_2 cannot be accurately calculated using DFT, we make the following approximation:

$$G_{O_2} = (2G_{H_2O} - 2G_{H_2} - 4.92\ eV) \quad (S7)$$

In addition, we also performed thermodynamic corrections on the adsorption state free energy:[3]

$$G(U) = E(U) + E_{ZPE} - T * S \quad (S8)$$

Finally, the reaction free energy of OER and ORR can be expressed as:

$$\Delta G_1(U) = G_{*OOH}(U) - [\frac{1}{2}G_{H_2} - e * U + G_*(U) + G_{O_2}] \quad (S9)$$

$$\Delta G_2(U) = [G_{*O}(U) + G_{H_2O}] - [\frac{1}{2}G_{H_2} - e * U + G_{*OOH}(U)] \quad (S10)$$

$$\Delta G_3(U) = G_{*OH}(U) - [\frac{1}{2}G_{H_2} - e * U + G_{*O}(U)] \quad (S11)$$

$$\Delta G_4(U) = [G_*(U) + G_{H_2O}] + [\frac{1}{2}G_{H_2} - e * U + G_{*OOH}(U)] \quad (S12)$$

Micro-kinetic method:

We assume that the reaction occurs with bare FePPc and FePPc with one coordination, and the reaction rate at the site is described by the reaction rate of the rate-limiting step. Therefore, the reaction rate can be written as:

$$R(U) = \sum k_i(U)[C_i(U)] \quad (S13)$$

$$k_i(U) = A_i \exp\left(\frac{-E_{a,i}}{k_B T}\right) \exp\left(\frac{-G_i^b(U)}{k_B T}\right) \quad (S14)$$

$R(U)$ is the total reaction rate, $C_i(U)$ is the concentration of various possible active sites. $A_i, E_{a,i}$ are effective pre-exponential factor and activation energy, which can be estimated to be 0.26 eV and 1.23×109 s^{-1}. k_B is Boltzmann constant. $k_i(U)$ are the reaction rates in corresponding active sites. This can be computed from Eq. S14, based on classical transition theory. $G_i\ b(U)$ is the reaction barrier.[4] In addition, the concentration $C_i(U)$ is balanced according to total site concentration following the formula:

$$[M] = \sum [C_i(U)] \quad (S15)$$

where M is total concentration of active sites, which can be computed by active sites divided by surface area. Besides, $C_i(U)$ follow the equilibrium constants:

$$K_i(U) = \frac{C_i(U)}{C_0(U)} = \exp\left(\frac{-G_i^f(U)}{KT}\right) \quad (S16)$$

$C_0(U)$ is concentration of $FePPc^{IS}$, the $G_ib(U)$ is formation energy of various active site relative to $FePPc^{IS}$. Finally, the current density can be calculated as:

$$j(U) = \frac{nFR(U)}{N_A} \quad (S17)$$

Where n is the charge transfer of reaction, F is Faraday constant, and N_A is the Avogadro constant. It should be noted that there is a limit to the reaction rate of ORR due to the solubility limit of oxygen. The reaction rate changes to:

$$k_i(U) = \rho_{Fe} \exp\left(\frac{-E_{a,i}}{k_BT}\right) \min\left(A_i \exp\left(\frac{-G_i^b(U)}{k_BT}\right), v_{o_2}\right) \quad (S18)$$

The values of v_{o_2} is taken as 1×10^8 s^{-1}. The ρ_{Fe} in our simulation model is set to 2.10E+13 cm^{-2}, corresponding to the experimental loadings about 3% wt.[5]

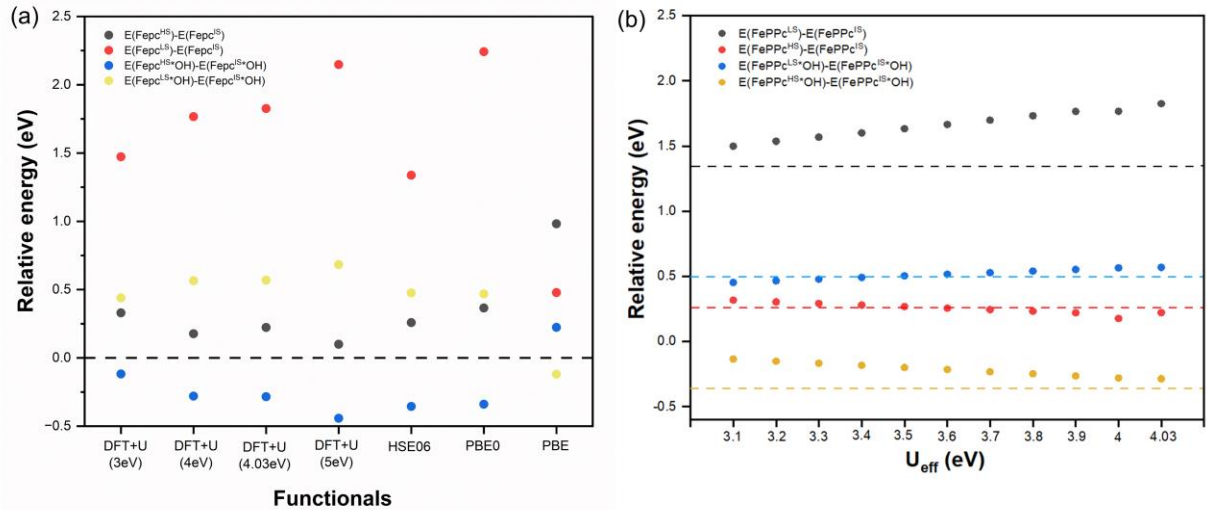

Fig. S1 (a) Comparison of IS/HS and LS/IS relative energy from hybrid functional calculations and DFT+U; (b) Relative energy obtained from DFT+U with different U values.

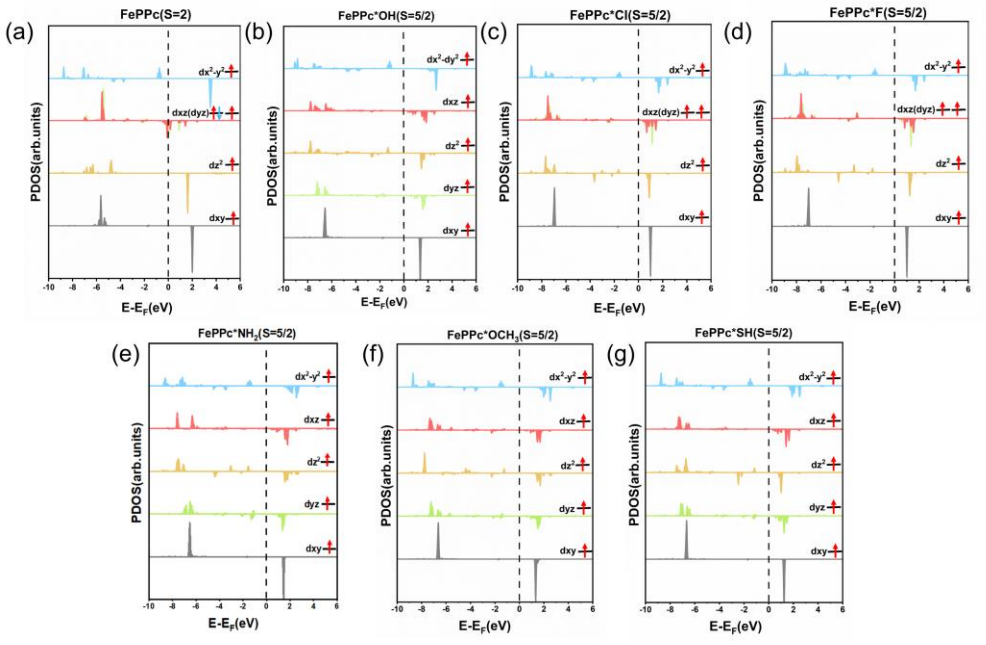

Fig. S2 PDOS and corresponding electronic configurations of HS FePPc and X-FePPc(X= OH/Cl/F/NH_2/OCH_3/SH).

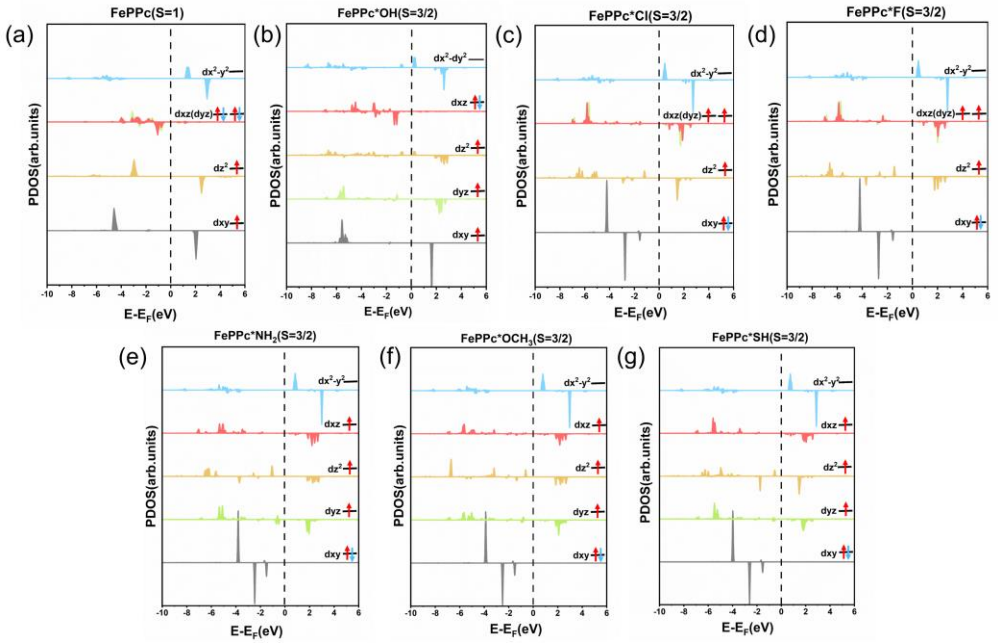

Fig. S3 PDOS and corresponding electronic configurations of IS FePPc and X-FePPc(X= OH/Cl/F/NH_2/OCH_3/SH).

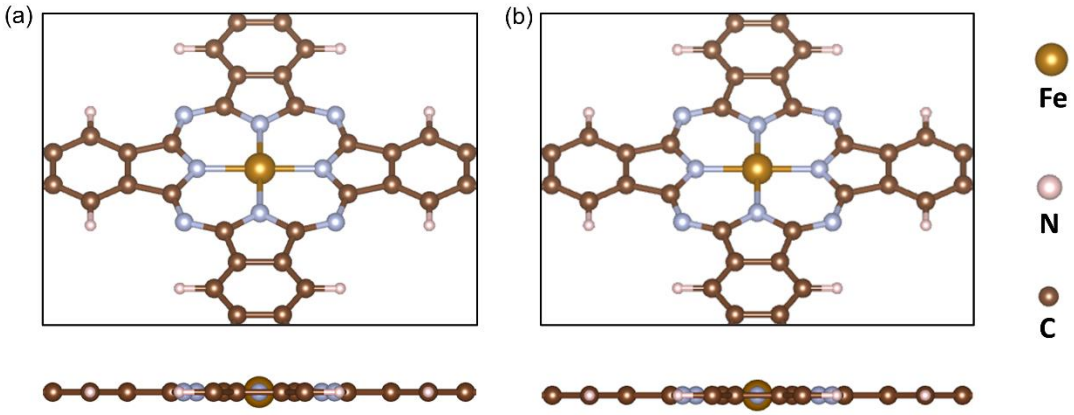

Fig. S4 The FePPc models for different spin states.(a)$FePPc^{HS}$, (b) $FePPc^{IS}$. The golden, gray, and brown balls represent Fe, C, and N atoms, respectively.

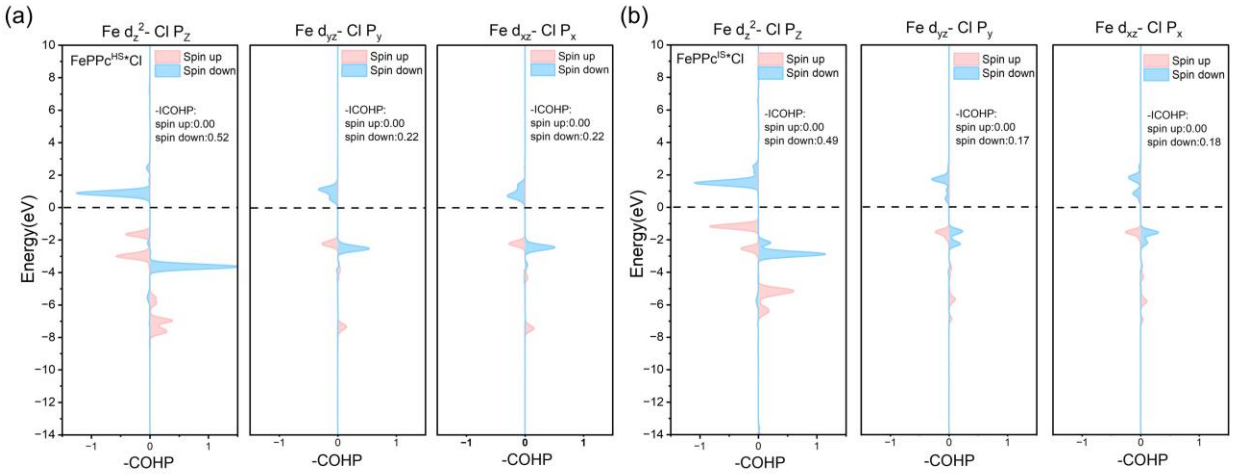

Fig. S5 Orbital resolved COHP analyze for the Fe-Cl bond in FePPc*Cl. (a) HS, (b) IS.

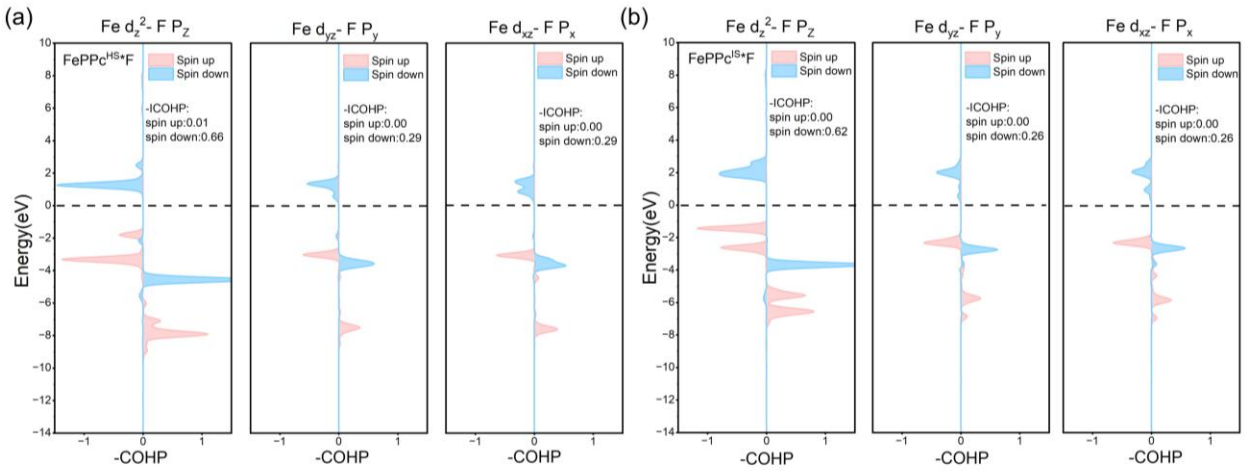

Fig. S6 Orbital resolved COHP analyze for the Fe-F bond in FePPc*F. (a) HS, (b) IS.

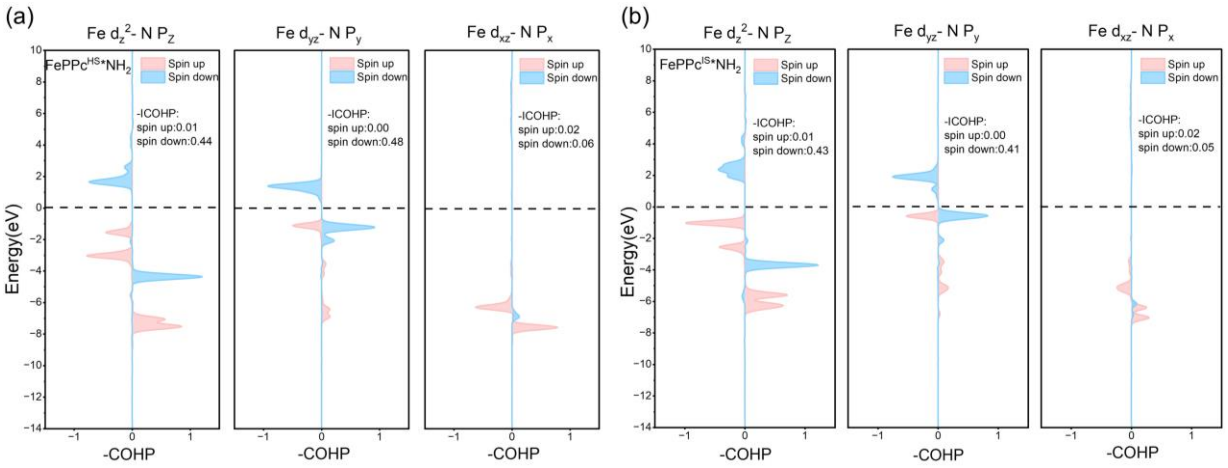

Fig. S7 Orbital resolved COHP analyze for the Fe-F bond in FePPc*NH_2. (a) HS, (b) IS.

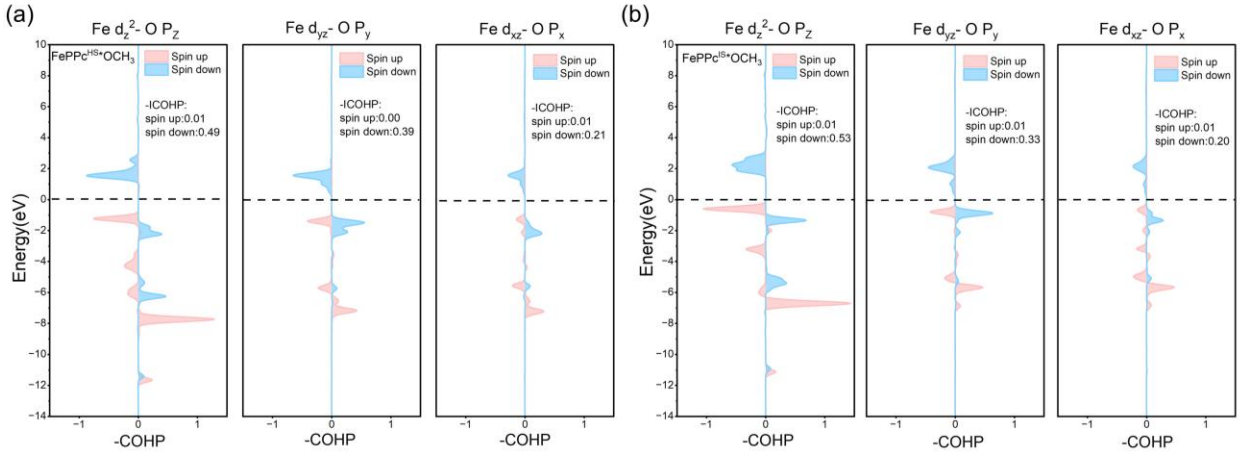

Fig. S8 Orbital resolved COHP analyze for the Fe-F bond in FePPc*OCH_3. (a) HS, (b) IS.

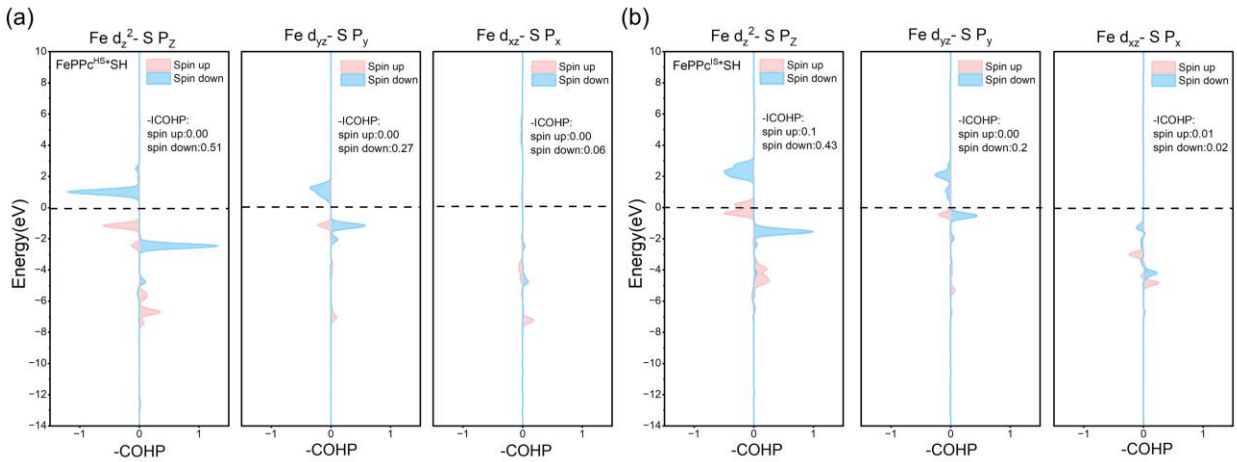

Fig. S9 Orbital resolved COHP analyze for the Fe-F bond in FePPc*NH_2. (a) HS, (b) IS.

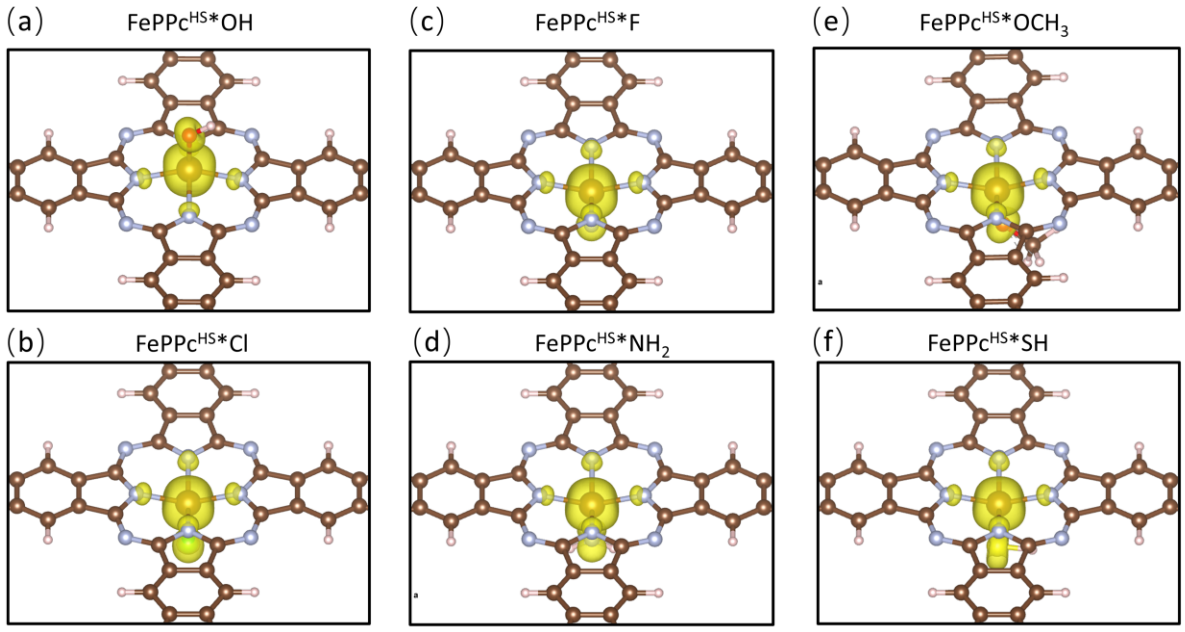

Fig. S10 Spin density of (a) FePPc^{HS}*OH, (b) FePPc^{HS}*Cl, (c) FePPc^{HS}*F, (d) FePPc^{HS}*NH_2, (e) FePPc^{HS}*OCH_3, (f) FePPc^{HS}*SH. (Isosurface: 0.01e/ bohr3)

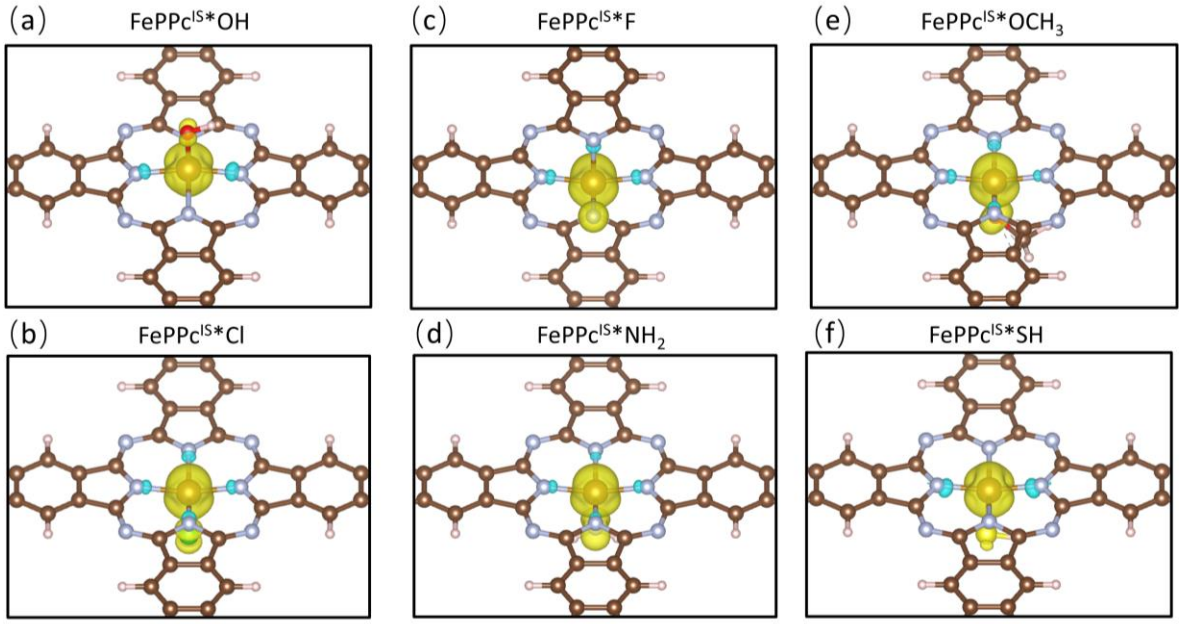

Fig. S11 Spin density of (a) FePPc^{IS}*OH, (b) FePPc^{IS}*Cl, (c) FePPc^{IS}*F, (d) FePPc^{IS}* NH_2, (e) FePPc^{IS}*OCH_3, (f) FePPc^{IS}*SH. (Isosurface: 0.01e/ bohr3)

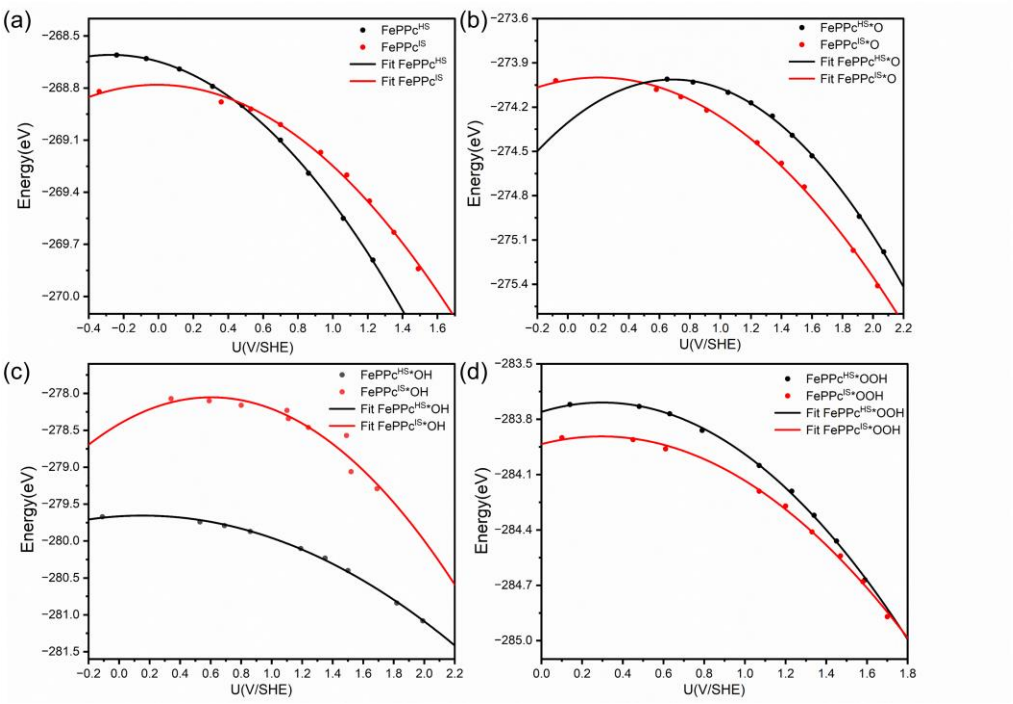

Fig. S12 Free energy of high spin and intermediate spin at different potential and fit curves. (a) FePPc, (b) FePPc*O, (c) FePPc*OH, (d) FePPc*OOH.

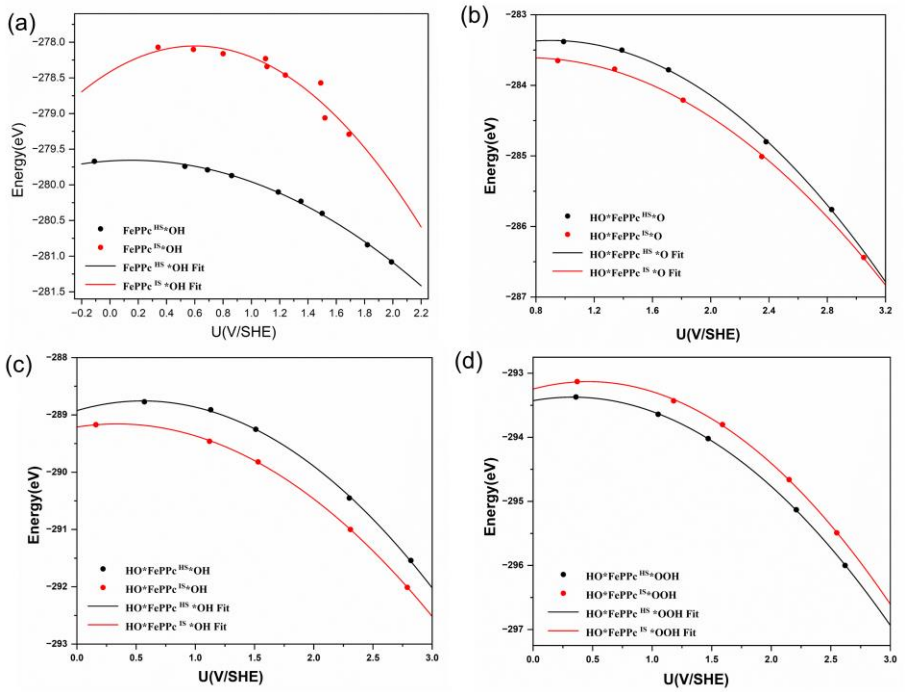

Fig. S13 Free energy of high spin and intermediate spin at different potential and fit curves. (a) FePPc*OH, (b) HO*FePPc*O, (c) HO*FePPc*OH, (d) HO*FePPc*OOH.

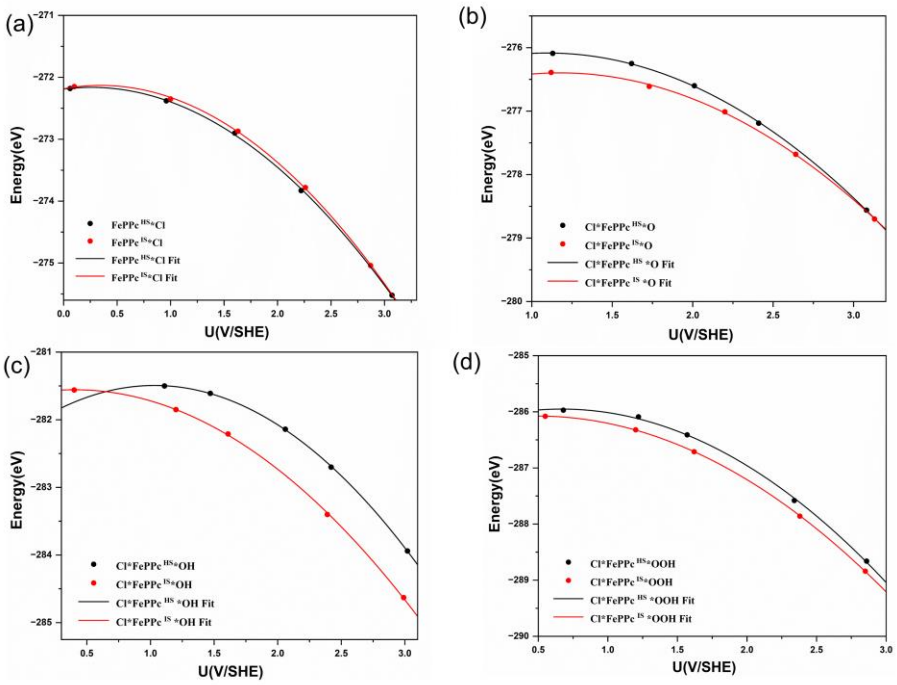

Fig. S14 Free energy of high spin and intermediate spin at different potential and fit curves. (a) FePPc*Cl, (b) Cl*FePPc*O, (c) Cl*FePPc*OH, (d) Cl*FePPc*OOH.

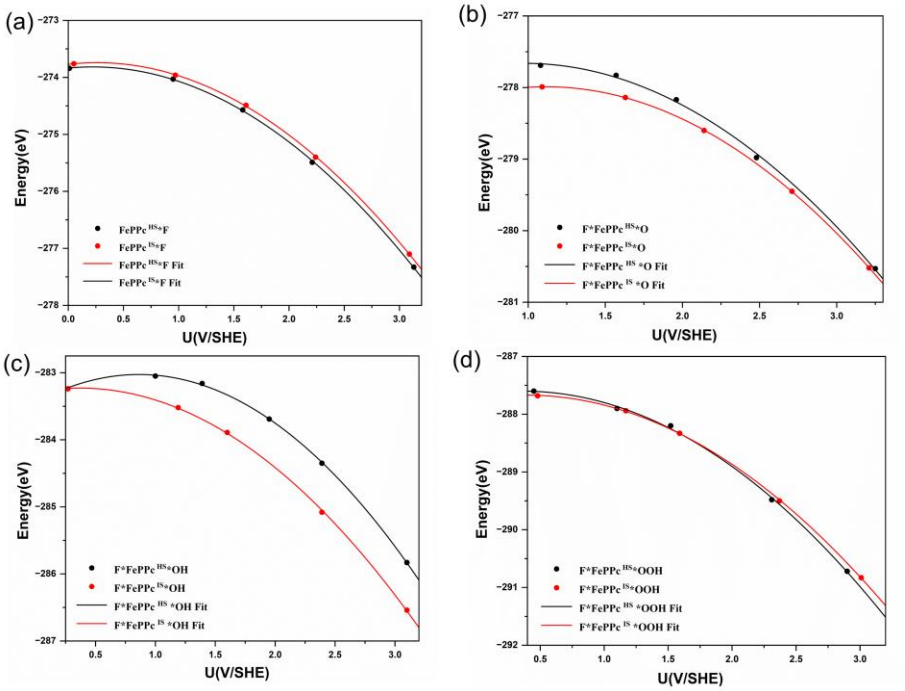

Fig. S15 Free energy of high spin and intermediate spin at different potential and fit curves. (a) FePPc*F, (b) F*FePPc*O, (c) F*FePPc*OH, (d) F*FePPc*OOH.

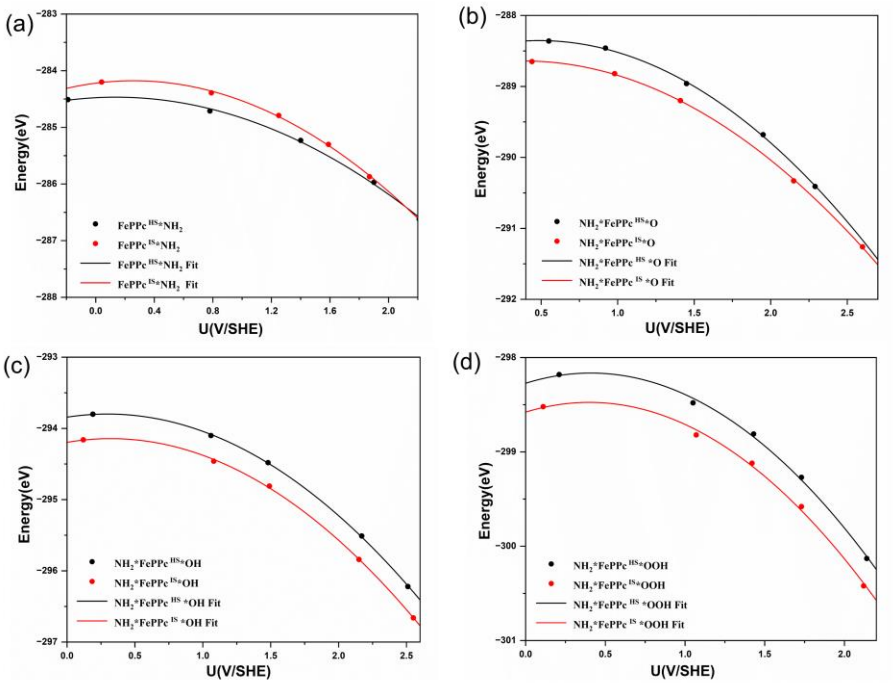

Fig. S16 Free energy of high spin and intermediate spin at different potential and fit curves. (a) FePPc*NH_2, (b) NH_2*FePPc*O, (c) NH_2*FePPc*OH, (d) NH_2*FePPc*OOH.

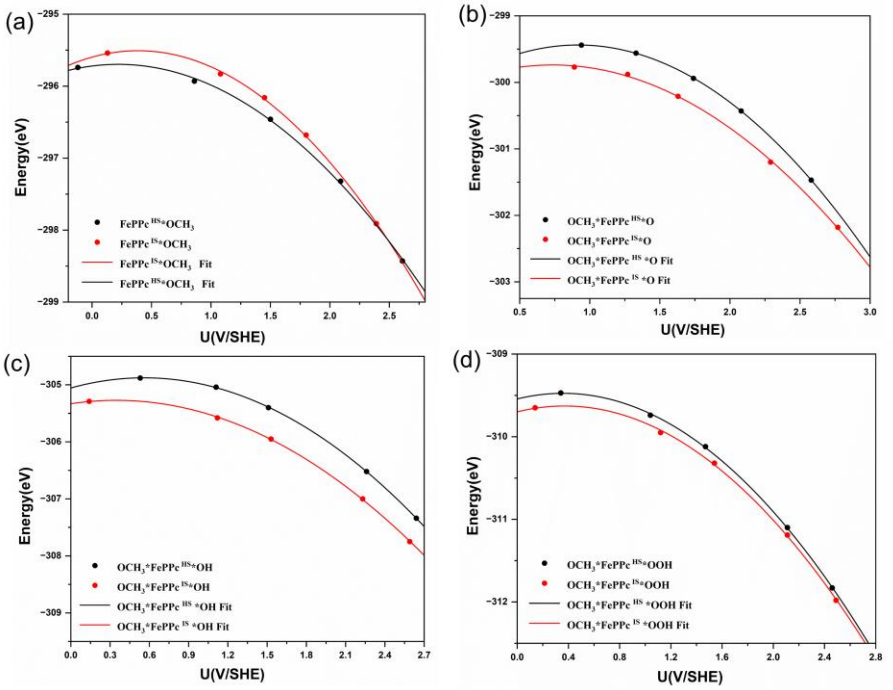

Fig. S17 Free energy of high spin and intermediate spin at different potential and fit curves. (a) FePPc*OCH_3, (b) OCH_3*FePPc*O, (c) OCH_3*FePPc*OH, (d) OCH_3*FePPc*OOH.

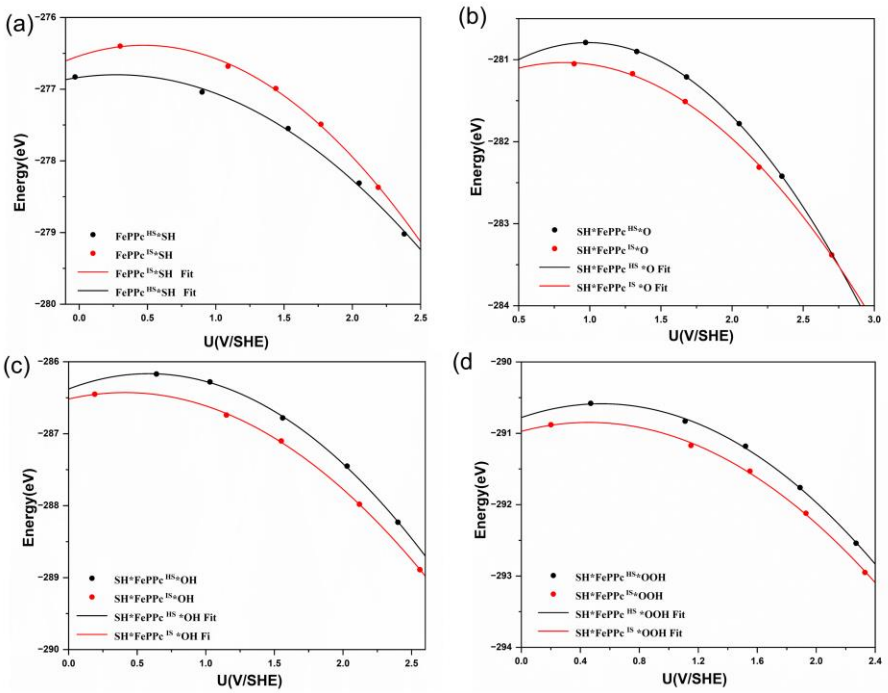

Fig. S18 Free energy of high spin and intermediate spin at different potential and fit curves. (a) FePPc*SH, (b) SH*FePPc*O, (c) SH*FePPc*OH, (d) SH*FePPc*OOH.

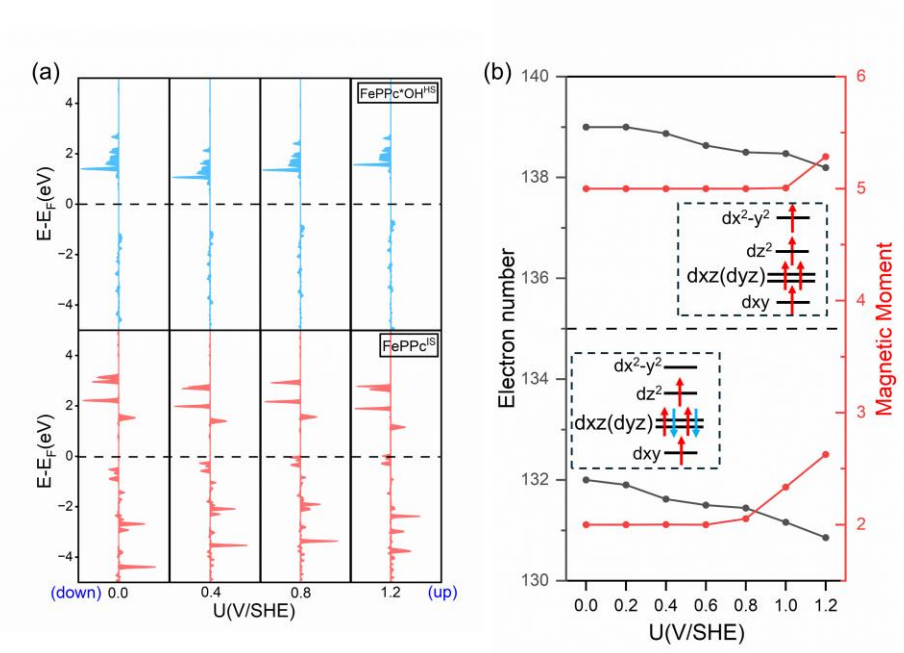

Fig. S19 (a) PDOS of the d orbitals of the $FePPc^{HS}$*OH (above) and $FePPc^{IS}$ (below); (b) change of electron number and magnetic moment (inserted panel: electron occupation diagram) with the voltage increase.

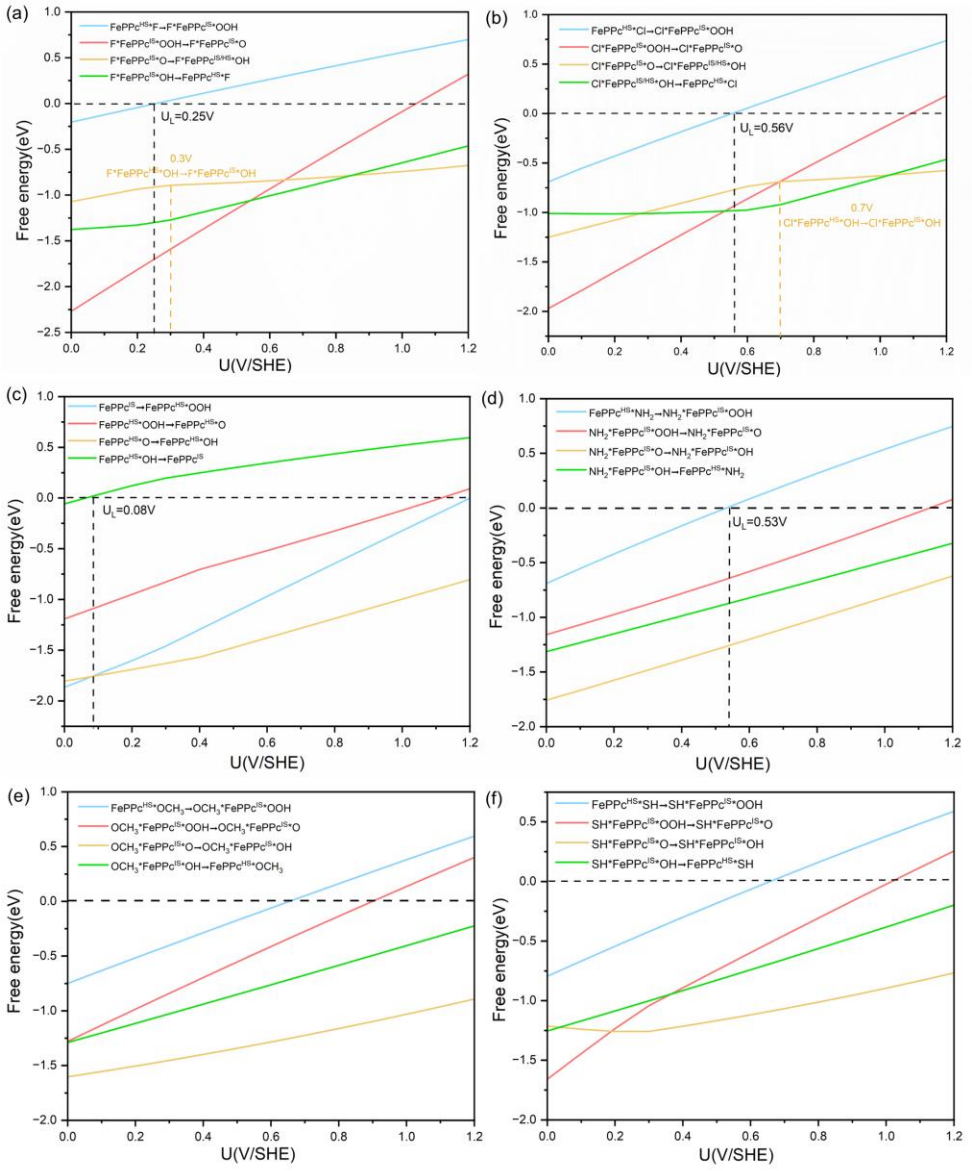

Fig. S20 ORR reaction free energy in (a) FePPc, (b) FePPc*Cl, (c) FePPc*F, (d) FePPc*NH_2, (e) FePPc*OCH_3, (f) FePPc*SH.

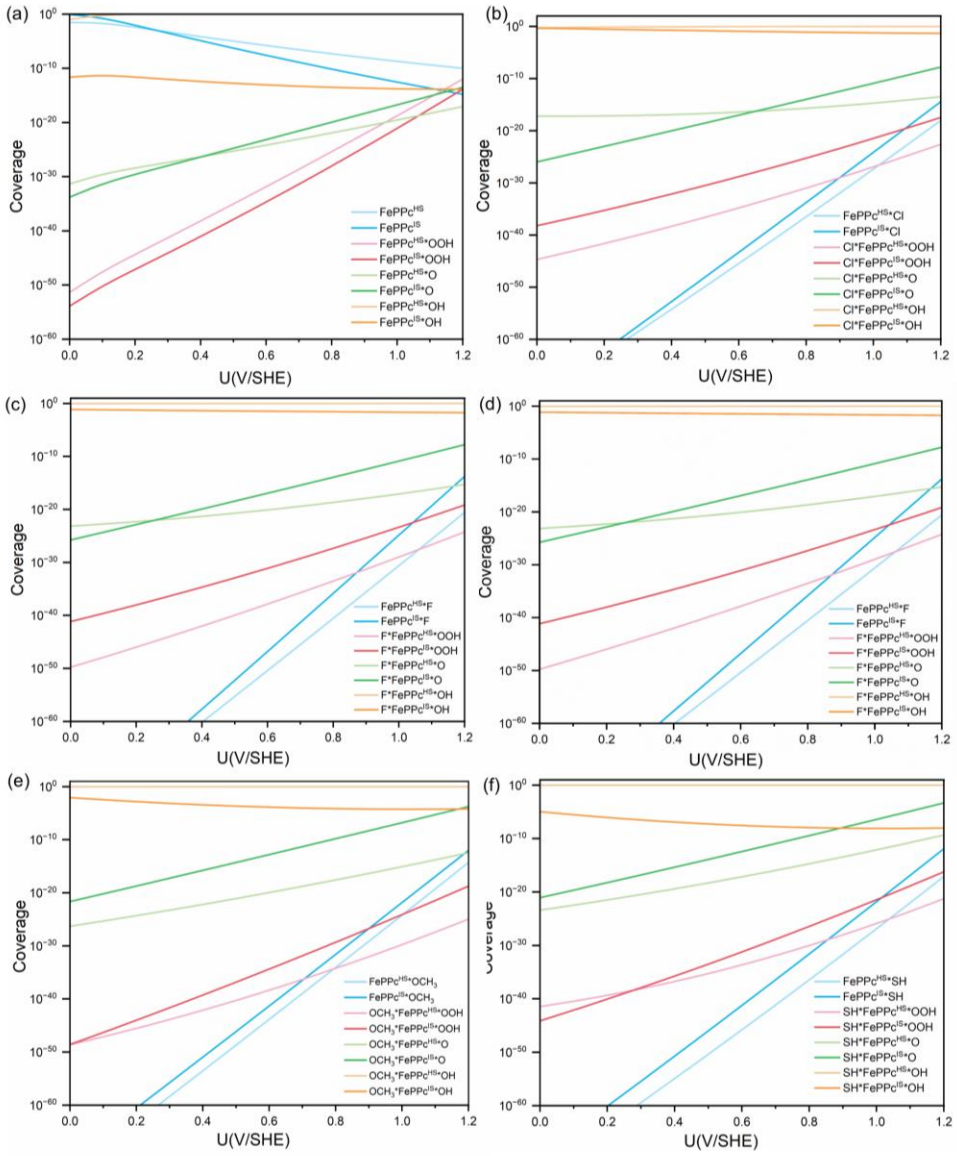

Fig. S21 Coverages of reaction intermediates. (a) FePPc*OH, (b) FePPc*Cl, (c) FePPc*F, (d) FePPc*NH_2, (e) FePPc*OCH_3, (f) FePPc*SH.

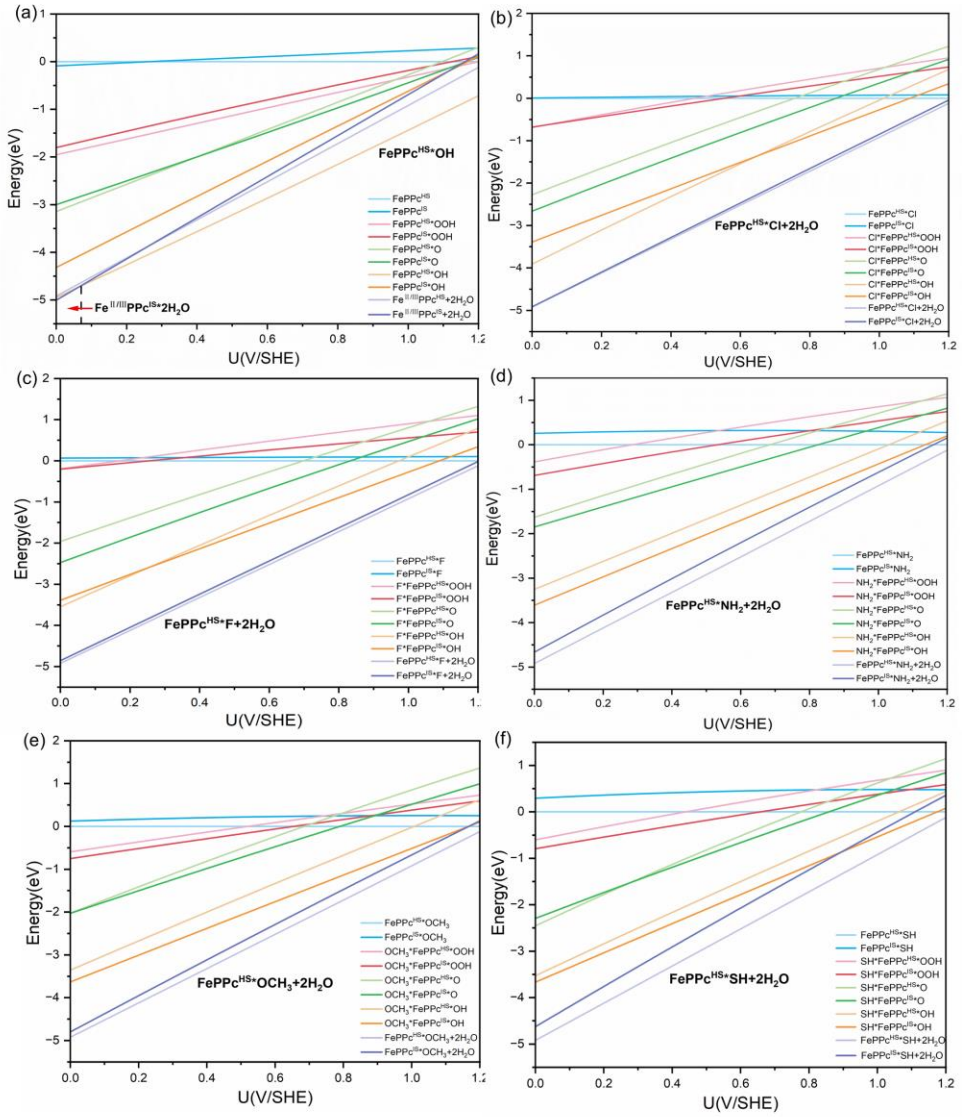

Fig. S22 Relative energy on different voltage (a) FePPc*OH, (b) FePPc*Cl, (c) FePPc*F, (d) FePPc*NH_2, (e) FePPc*OCH_3, (f) FePPc*SH.

Table S1. Test of k-point sampling for structural optimization.

G^*_{OH}(eV)	$FePPc^{HS}$*OH	$FePPc^{IS}$*OH
ΔG_{3x3x1}-ΔG_{2x2x1}	0.08	0.01
ΔG_{4x4x1}-ΔG_{2x2x1}	0.08	0.01

Table S2. Total energy and structural parameters of FePPc and X-FePPc with two coordination in neutral state.

model	E(eV)	Fe-N(Å)	dFe(Å)
$FePPc^{HS}$	-268.17	2.00	0
$FePPc^{IS}$	-268.47	1.97	0
$FePPc^{HS}$*OH	-278.96	2.06	0.54
$FePPc^{IS}$*OH	-278.15	2.02	0.36
$FePPc^{HS}$*Cl	-271.90	2.05	0.51
$FePPc^{IS}$*Cl	-271.74	2.00	0.29
$FePPc^{HS}$*F	-273.44	2.05	0.52
$FePPc^{IS}$*F	-273.25	2.00	0.29
$FePPc^{HS}$*NH_2	-283.66	2.06	0.53
$FePPc^{IS}$*NH_2	-283.34	2.00	0.29
$FePPc^{HS}$*OCH_3	-294.43	2.06	0.45
$FePPc^{IS}$*OCH_3	-294.17	2.00	0.21
$FePPc^{HS}$*SH	-276.39	2.05	0.51
$FePPc^{IS}$*SH	-276.20	1.99	0.27

Table S3. Total energy and structural parameters of FePPc and X-FePPc with in neutral state.

model	Spin	E(eV)	model	Spin	E(eV)
$FePPc^{HS}$*OH	5/2	-278.96	$FePPc^{HS}$*Cl	5/2	-271.90
$FePPc^{IS}$*OH	3/2	-278.15	$FePPc^{IS}$*Cl	3/2	-271.74

model	Spin	E(eV)	model	Spin	E(eV)
HO*FePPc^{HS}*O	2	-282.42	O*FePPc^{HS}*Cl	2	-275.47
HO*FePPc^{IS}*O	1	-282.71	O*FePPc^{IS}*Cl	1	-275.71
HO*FePPc^{HS}*OH	5/2	-287.64	HO*FePPc^{HS}*Cl	5/2	-280.60
HO*FePPc^{IS}*OH	1	-287.45	HO*FePPc^{IS}*Cl	1	-280.85
HOO*FePPc^{HS}*OH	5/2	-292.02	HOO*FePPc^{HS}*Cl	5/2	-285.00
HOO*FePPc^{IS}*OH	1	-291.82	HOO*FePPc^{IS}*Cl	1	-285.16
FePPc^{HS}*F	5/2	-273.44	FePPc^{HS}*NH_2	5/2	-283.66
FePPc^{IS}*F	3/2	-273.25	FePPc^{IS}*NH_2	3/2	-283.34
O*FePPc^{HS}*F	2	-276.93	O*FePPc^{HS}*NH_2	2	-287.10
O*FePPc^{IS}*F	1	-277.18	O*FePPc^{IS}*NH_2	1	-287.41
HO*FePPc^{HS}*F	5/2	-282.10	HO*FePPc^{HS}*NH_2	2	-292.40
HO*FePPc^{IS}*F	1	-282.42	HO*FePPc^{IS}*NH_2	1	-292.76
HOO*FePPc^{HS}*F	5/2	-286.33	HOO*FePPc^{HS}*NH_2	2	-296.63
HOO*FePPc^{IS}*F	1	-286.38	HOO*FePPc^{IS}*NH_2	1	-296.97
FePPc^{HS}*OCH_3	5/2	-294.43	FePPc^{HS}*SH	5/2	-276.39
FePPc^{IS}*OCH_3	3/2	-294.17	FePPc^{IS}*SH	3/2	-276.20
O*FePPc^{HS}*OCH_3	2	-297.94	O*FePPc^{HS}*SH	2	-280.08
O*FePPc^{IS}*OCH_3	1	-298.28	O*FePPc^{IS}*SH	1	-280.38
HO*FePPc^{HS}*OCH_3	5/2	-303.17	HO*FePPc^{HS}*SH	5/2	-285.28
HO*FePPc^{IS}*OCH_3	1	-303.61	HO*FePPc^{IS}*SH	1	-285.60
HOO*FePPc^{HS}*OCH_3	5/2	-307.60	HOO*FePPc^{HS}*SH	2	-289.53
HOO*FePPc^{IS}*OCH_3	1	-307.88	HOO*FePPc^{IS}*SH	1	-289.86

Table S4. Total energy and structural parameters of FePPc with one coordination in neutral state.

model	E(eV)	Fe-N(Å)	dFe(Å)
O*FePPc^{HS}*OH	-282.792	2.01	-0.06
O*FePPc^{IS}*OH	-283.08	2.01	-0.03
HO*FePPc^{HS}*OH	-288.2	2.02	0
HO*FePPc^{IS}*OH	-288.63	1.98	0
HOO*FePPc^{HS}*OH	-292.71	2.03	0.33
HOO*FePPc^{IS}*OH	-292.51	1.99	0.02
O*FePPc^{HS}*Cl	-275.51	2.01	0.12
O*FePPc^{IS}*Cl	-275.75	1.98	0.08
HO*FePPc^{HS}*Cl	-280.87	2.02	0.07
HO*FePPc^{IS}*Cl	-281.12	1.99	0.03
HOO*FePPc^{HS}*Cl	-285.31	2.02	-0.19
HOO*FePPc^{IS}*Cl	-285.47	1.99	-0.05
O*FePPc^{HS}*F	-277.03	2.01	0.10
O*FePPc^{IS}*F	-277.28	1.98	0.07
HO*FePPc^{HS}*F	-282.42	2.02	0.03
HO*FePPc^{IS}*F	-282.74	1.99	0.03
HOO*FePPc^{HS}*F	-286.98	2.03	-0.34
HOO*FePPc^{IS}*F	-287.04	1.99	-0.03
O*FePPc^{HS}*NH_2	-287.73	2.02	0.08
O*FePPc^{IS}*NH_2	-288.04	1.98	0.04
HO*FePPc^{HS}*NH_2	-293.29	2.02	0.11
HO*FePPc^{IS}*NH_2	-293.65	1.99	0.03
HOO*FePPc^{HS}*NH_2	-297.6	2.01	-0.11
HOO*FePPc^{IS}*NH_2	-297.93	1.98	-0.04

model	E(eV)	Fe-N(Å)	dFe(Å)
$O*FePPc^{HS}*OCH_3$	-298.96	2.01	0.13
$O*FePPc^{IS}*OCH_3$	-299.31	1.98	0.11
$HO*FePPc^{HS}*OCH_3$	-304.41	2.02	0.01
$HO*FePPc^{IS}*OCH_3$	-304.85	1.98	0.09
$HOO*FePPc^{HS}*OCH_3$	-308.86	2.03	-0.17
$HOO*FePPc^{IS}OCH_3$	-309.14	1.98	0.04
$O*FePPc^{HS}*SH$	-280.31	2.02	0.15
$O*FePPc^{IS}*SH$	-280.41	2.02	0.14
$HO*FePPc^{HS}*SH$	-285.7	2.02	0.15
$HO*FePPc^{IS}*SH$	-286.01	1.98	0.03
$HOO*FePPc^{HS}*SH$	-290.03	2.02	-0.06
$HOO*FePPc^{IS}*SH$	-290.36	1.98	-0.02

References:

1. J. K. Nørskov, J. Rossmeisl, A. Logadottir, L. Lindqvist, J. R. Kitchin, T. Bligaard and H. Jónsson, *The Journal of Physical Chemistry B*, 2004, **108**, 17886-17892.
2. I. C. Man, H.-Y. Su, F. Calle-Vallejo, H. A. Hansen, J. I. Martínez, N. G. Inoglu, J. Kitchin, T. F. Jaramillo, J. K. Nørskov and J. Rossmeisl, *ChemCatChem*, 2011, **3**, 1159-1165.
3. M. Li, L. Zhang, Q. Xu, J. Niu and Z. Xia, *Journal of Catalysis*, 2014, **314**, 66-72.
4. Y. Wang, Y.-J. Tang and K. Zhou, *Journal of the American Chemical Society*, 2019, **141**, 14115-14119.
5. J. Chen, M. Wang, L. Chen, K. Guo, B. Liu, K. Wang, N. Li, L. Bao and X. Lu, *Advanced Energy and Sustainability Research*, 2024, **5**, 2400010.